Materials
Advances

## Supporting information

# Succinate coprecipitation synthesized Cr-doped $Fe_2O_3$ as an efficient electrocatalyst for hydrogen evolution reaction in alkaline medium

Paulin Kammi Yontchoum [a,b], Carelle Martiale Kamga Meffo [a], Bilal Tasdemir [c], Kenneth Mbene [a], Cedrik Yonti Ngnintedem [a],

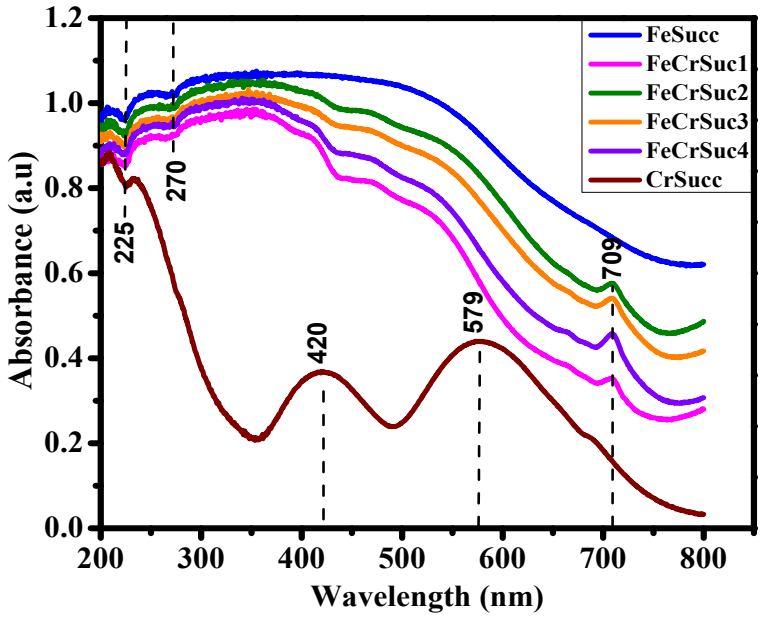


**Fig. S 1** UV-visible spectra of Cr succinate, Fe succinate and all the Cr-doped Fe succinate

Bilge Saruhan [c], Patrice Kenfack Tsobnang [d], Roussin Lontio Fomekong [a,*]

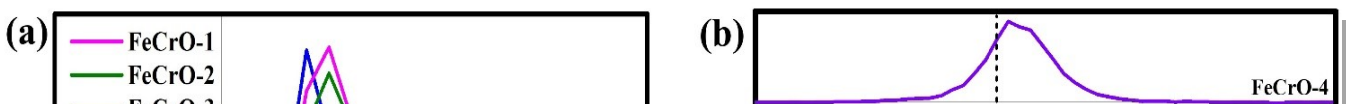

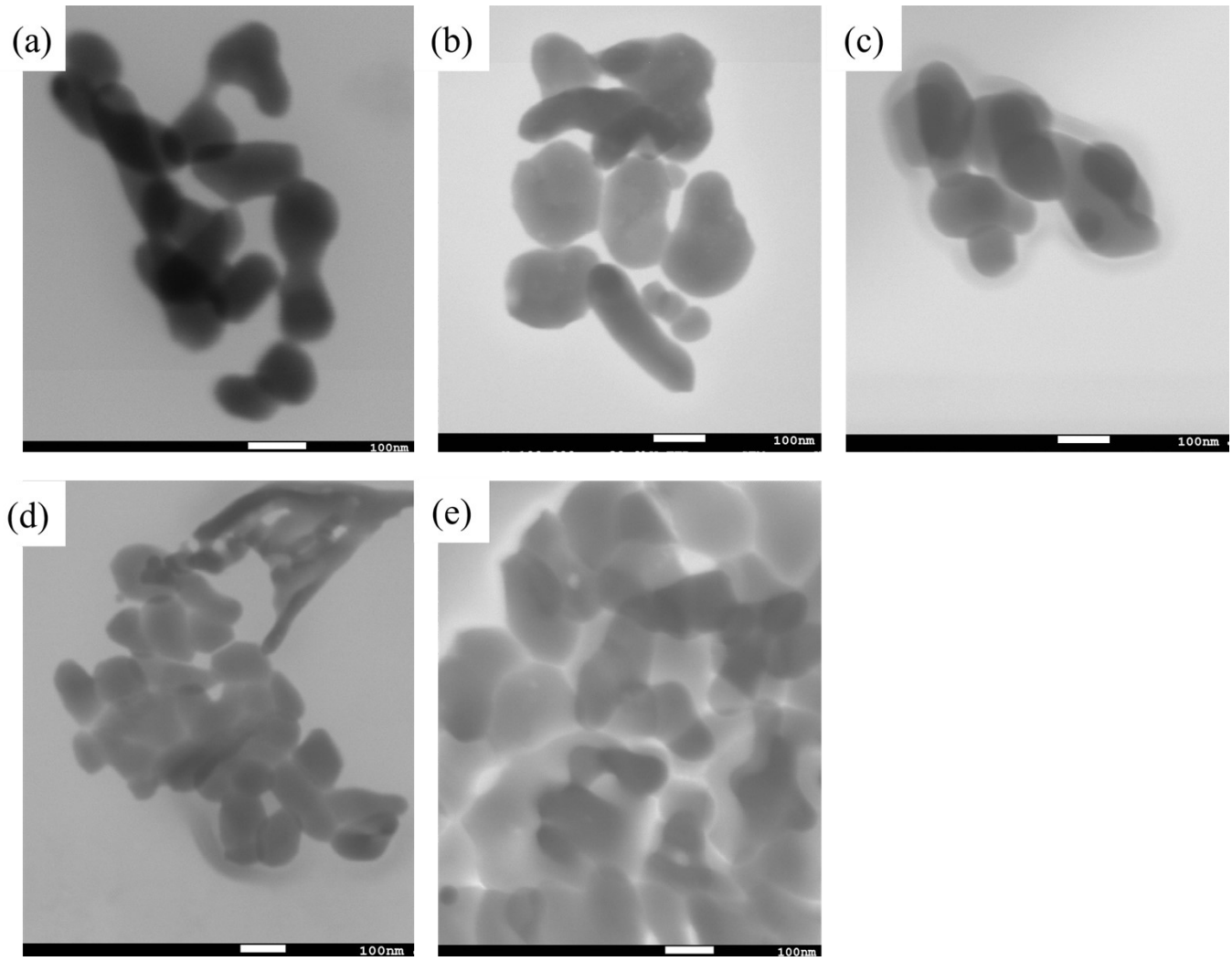


**Fig. S 3** STEM Images of (a) $Fe_2O_3$, (b) FeCrO-1, (c) FeCrO-2, (d) FeCrO-3, and (e) FeCrO-4.

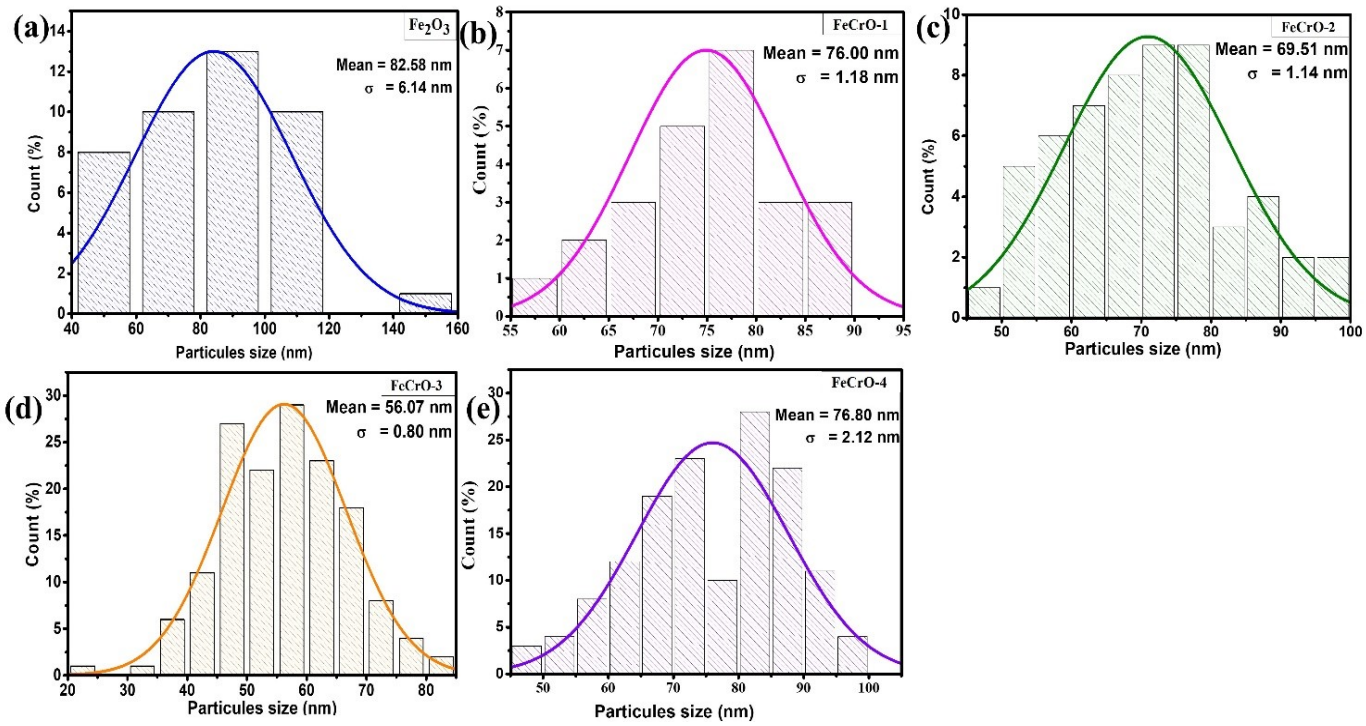


**Fig. S 4** Histogram of particle size distribution with their average particle size**.** (a) $Fe_2O$, (b) FeCrO-1, (c) FeCrO-2, (d) FeCrO-3, (e) FeCrO-4

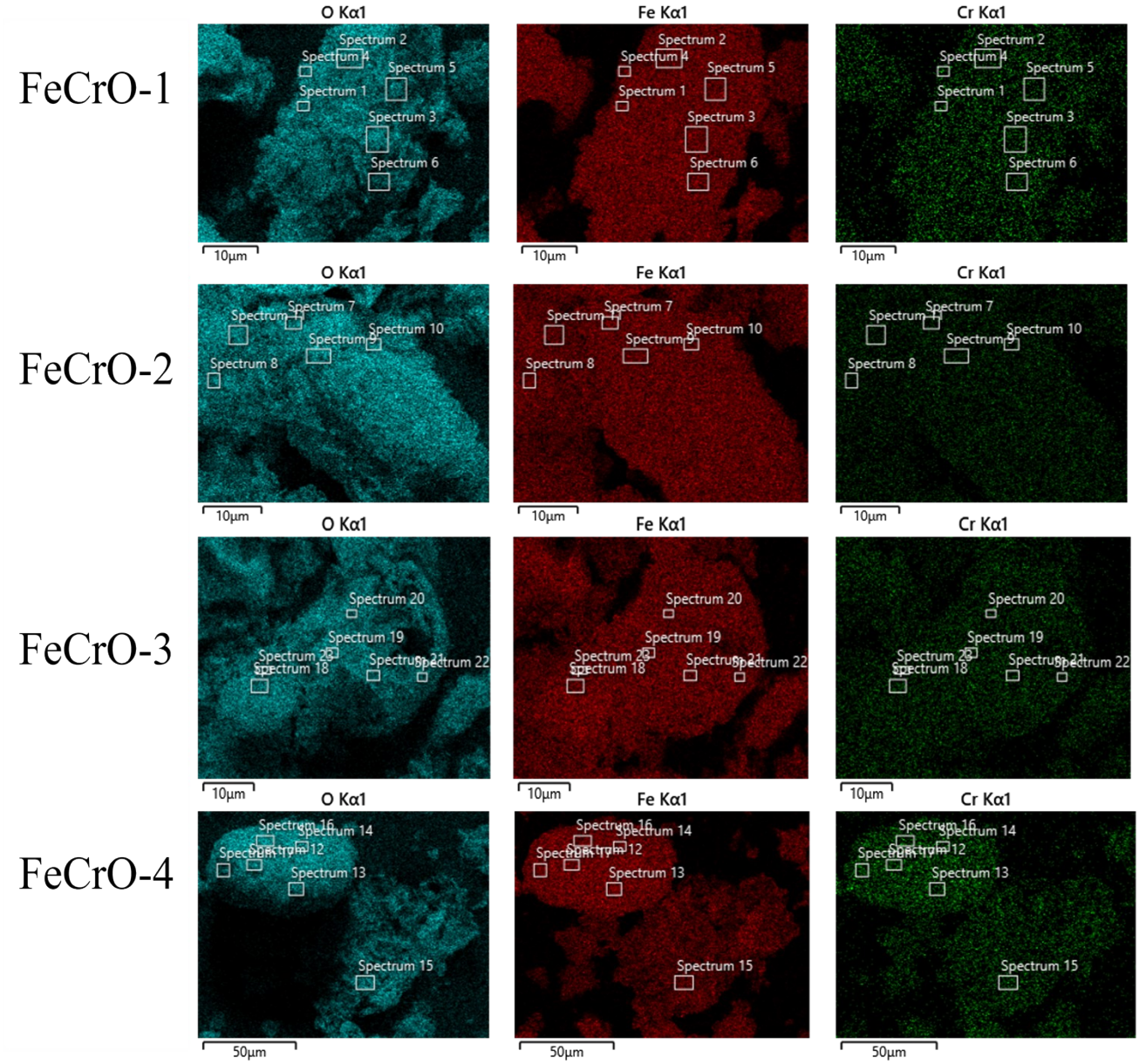


**Fig. S 5** Elemental mapping of all the Cr-doped $Fe_2O_3$ (FeCrO-1, FeCrO-2, FeCrO-3 and FeCrO-4)

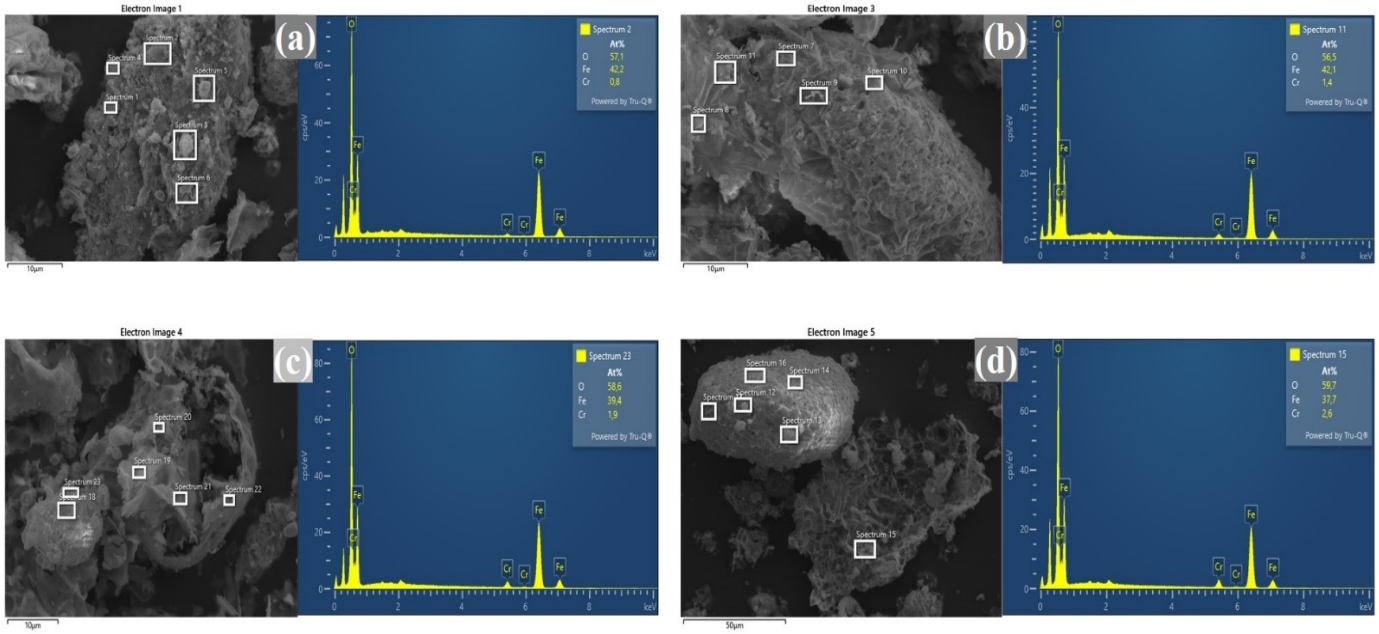


**Fig. S 6** EDX spectra with associated SEM images of (a) FeCrO-1, (b) FeCrO-2, (c) FeCrO-3 and (d) FeCrO-4

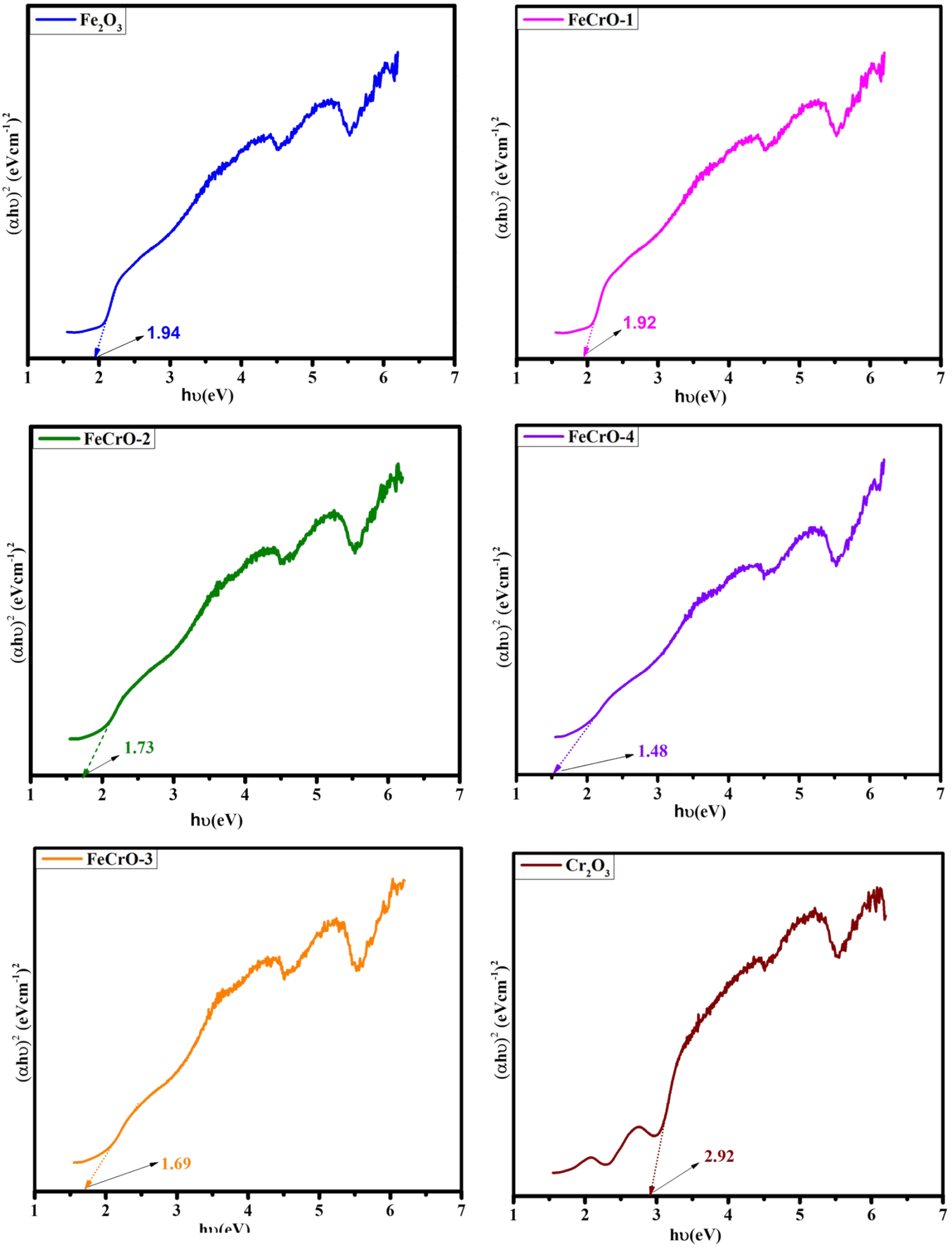


**Fig. S 7** The Tauc Plots, $(F(R)*hv)^2$ versus hv, of metal oxides


**Fig. S 8** Images of metal oxides samples. (a) $Fe_2O_3$, (b) $Cr_2O_3$, (c) FeCrO-1, (d) FeCrO-2, (e) FeCrO-3, (f) FeCrO-4

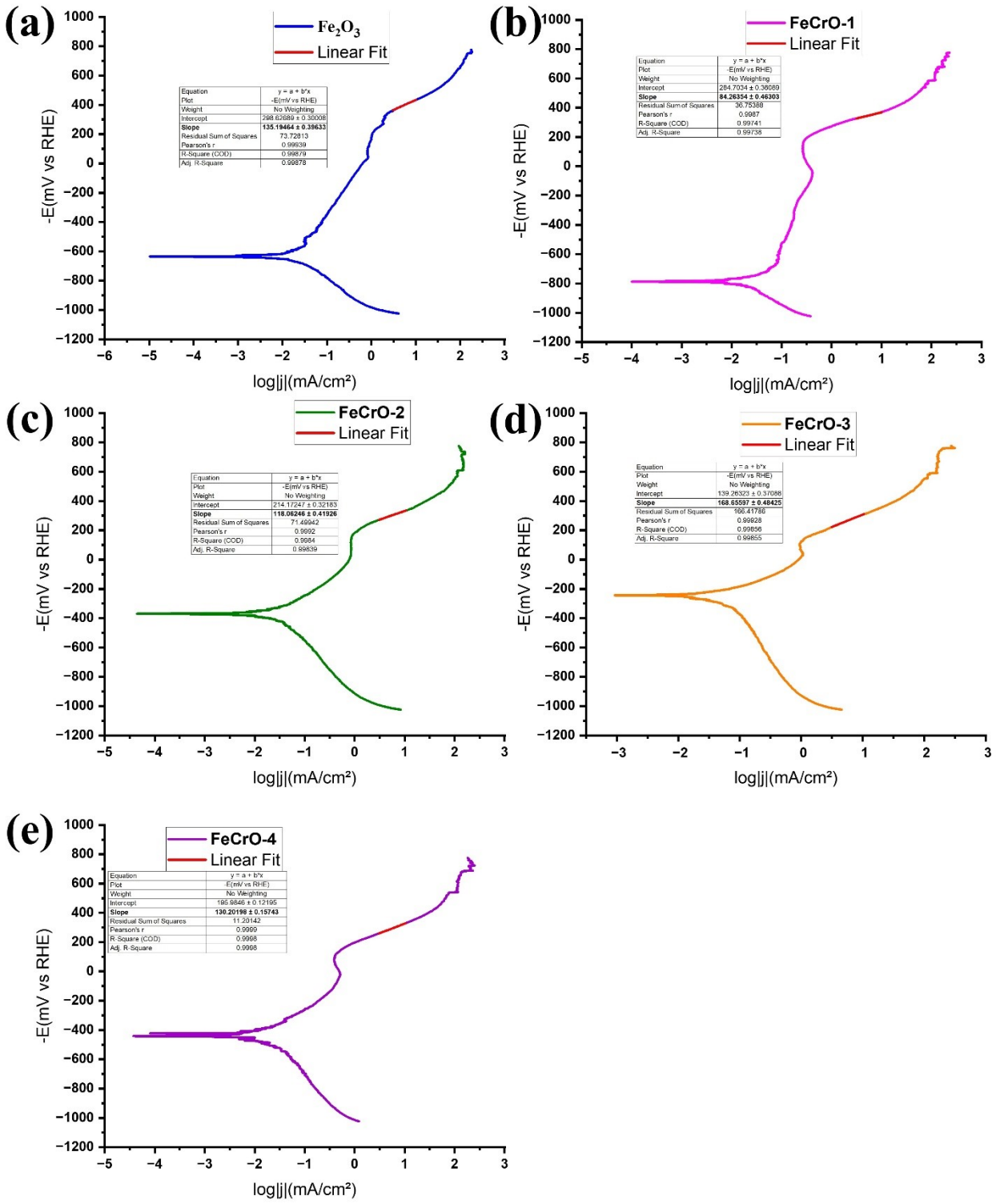


**Fig. S 9** Tafel plot derived from the LSV curves: (a) $Fe_2O_3$, (b) FeCrO-1, (c) FeCrO-2, (d) FeCrO-3, (e) FeCrO-4

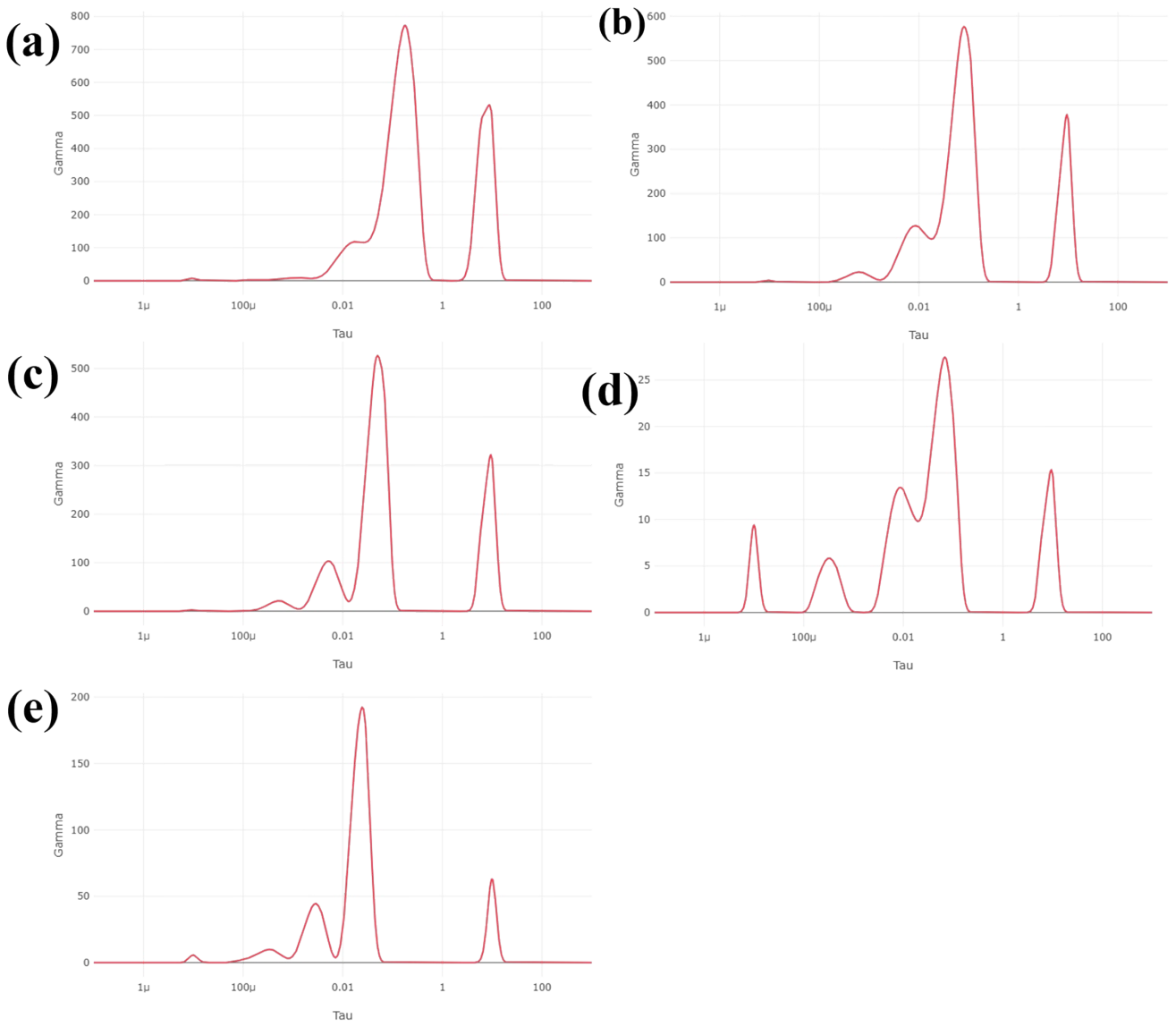


**Fig. S 10** Distribution of Relaxation Times (DTR) analysis: (a) $Fe_2O_3$, (b) FeCrO-1, (c) FeCrO-2, (d) FeCrO-3, (e) FeCrO-4) (This DRT implementation is based on ideas and methods introduced by the Ciucci group[1])

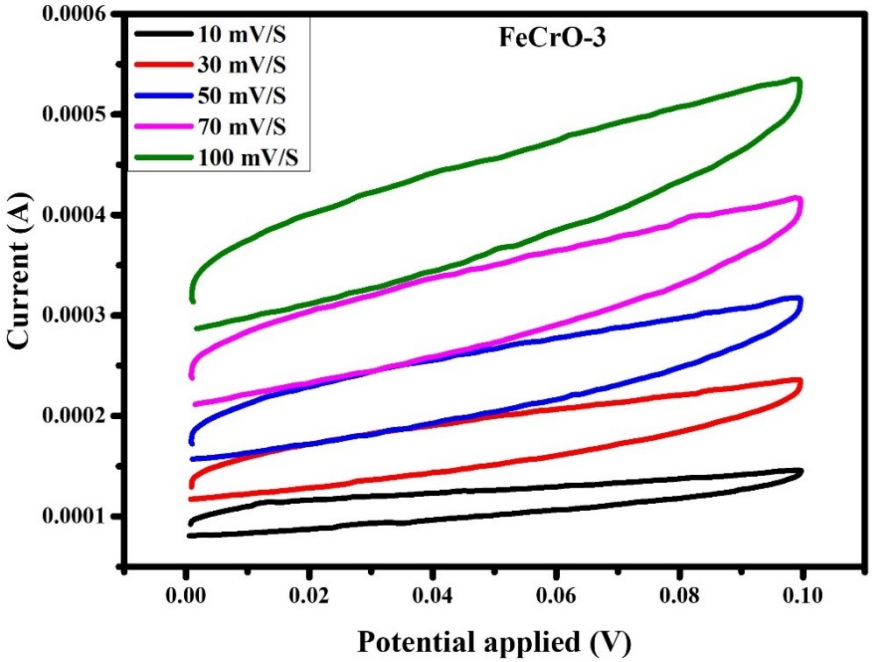


**Fig. S 11** CV at different scan rates of the 5.5 a% Cr-doped $Fe_2O_3$

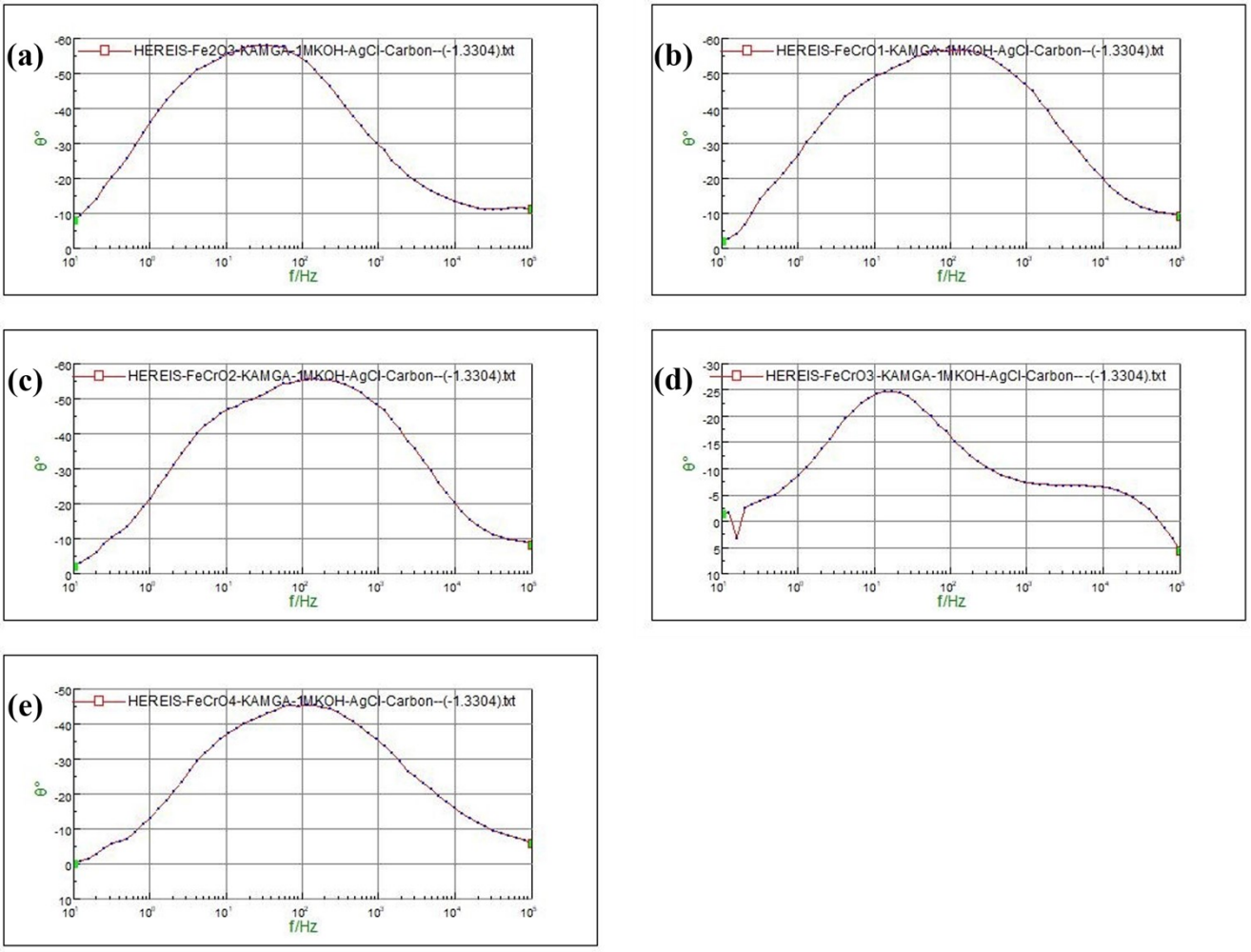


**Fig. S 12** Bode plot: (a) $Fe_2O_3$, (b) FeCrO-1, (c) FeCrO-2, (d) FeCrO-3, (e) FeCrO-4)

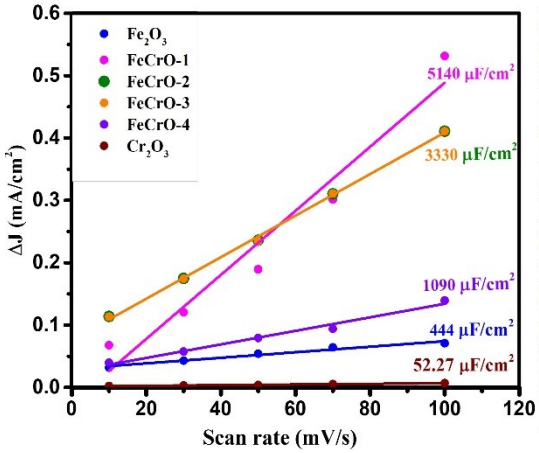


| Equation | y = a + b*x | | | | | |
|---|---|---|---|---|---|---|
| **Plot** | **Fe2O3** | **FeCrO-1** | **FeCrO-2** | **FeCrO-3** | **FeCrO-4** | **Cr2O3** |
| Weight | No Weighting | | | | | |
| Intercept | 0.02979 ± 0.00281 | -0.02487 ± 0.04042 | 0.07657 ± 0.0042 | 0.0757 ± 0.00462 | 0.02562 ± 0.00492 | 0.00161 ± 1.46645E-4 |
| **Slope (F/cm2)** | **4.44098E-4 ± 4.62959E-5** | **0.00514 ± 6.66283E-4** | **0.00332 ± 6.92507E-5** | **0.00333 ± 7.61926E-5** | **0.00109 ± 8.10442E-5** | **5.22746E-5 ± 2.41738E-6** |
| Residual Sum of Squares | 3.1378E-5 | 0.0065 | 7.02085E-5 | 8.49899E-5 | 9.61579E-5 | 8.5552E-8 |
| Pearson's r | 0.98409 | 0.97567 | 0.99935 | 0.99922 | 0.99174 | 0.99681 |
| R-Square (COD) | 0.96843 | 0.95193 | 0.9987 | 0.99843 | 0.98354 | 0.99363 |
| Adj. R-Square | 0.9579 | 0.93591 | 0.99826 | 0.99791 | 0.97806 | 0.9915 |

**Fig. S 13** Linear regression analysis of the scan rate dependence of current densities at 0.05 V for pristine $Fe_2O_3$, $Cr_2O_3$ and Cr-doped $Fe_2O_3$

1. T. H. Wan, M. Saccoccio, C. Chen and F. Ciucci, *Electrochimica Acta*, 2015, **184**, 483-499.